JOURNAL OF CLIMATOLOGY, VOL. 5, 589–606 (1985) 551.579:551.582(4/9):556

# CLIMATOLOGY OF THE TERRESTRIAL SEASONAL WATER CYCLE

CORT J. WILLMOTT AND CLINTON M. ROWE
*Center for Climatic Research, Department of Geography, University of Delaware, Newark, Delaware 19716, U.S.A.*

AND

YALE MINTZ
*Department of Meteorology, University of Maryland, College Park, Maryland 20742, U.S.A. and Laboratory for Atmospheres, NASA Goddard Space Flight Center, Greenbelt, Maryland 20771, U.S.A.*

*Received 15 January 1985*

## ABSTRACT

Calculations of the spatial and seasonal variations of the continental fields of snow-cover, soil moisture and evapotranspiration are presented and interpreted. The calculations were made with a water budget analysis that is based on observed average monthly precipitation and an estimate of potential evapotranspiration derived from observed average monthly surface temperature, using a modified version of the method of Thornthwaite. Monthly average water budget analyses were made for 13,332 stations over the globe and, then spatially interpolated to a regular grid at 1° by 1° latitude-longitude intervals. From the monthly fields on a 4° by 5° subset of the 1° by 1° grid, the annual mean and standard deviation as well as the first and second annual harmonics were extracted and are displayed on global maps. Of the three fields, soil moisture has the largest space–time variation; snow-cover the smallest variation; and evapotranspiration an intermediate level of variation.

KEY WORDS Water balance Evapotranspiration Soil moisture Snow-cover

## INTRODUCTION

### *Purpose*

Investigations of the climate system continue to be impeded by the paucity of reliable global water balance data. Monthly, seasonal and annual precipitation and air temperature data have been compiled (e.g. Möller, 1951; Wernstedt, 1972; Jaeger, 1976; Steinhauser, 1979; Willmott *et al.*, 1981; Spangler and Jenne, 1984), but no global precipitation or temperature data set gives entirely satisfactory space–time coverage of the continents. Recent reviews of global precipitation data by Mintz (1981) and Jaeger (1983) illustrate this problem. Monthly, seasonal and annual fields of evapotranspiration, soil moisture and snow-cover on the continents are even less well known. Baumgartner (1981), for instance, in his review of the large-scale water balance literature, makes it clear that 'worldwide water balances for shorter periods than a year are not available at the moment'. The true global water balance fields, none the less, are required for many climatological purposes, not the least important of which is the operational and scientific evaluation of global climate model (GCM) predictions of the water cycle. These fields may also be used as initial or boundary conditions by GCMs. Our purpose in this paper is to augment the store of empirically derived water budget information and to interpret the relationships among the water budget components.

0196–1748/85/060589–18$01.80
© 1985 by the Royal Meteorological Society

*Background*

About forty years ago, Thornthwaite (in Wilm *et al.*, 1944) proposed a relatively simple procedure for estimating land-surface evapotranspiration and soil moisture as well as other aspects of the terrestrial water cycle such as water surplus. Four years later, in his well-known paper 'An approach toward a rational classification of climate' (Thornthwaite, 1948), he gave a comprehensive description of the procedure and applied it. Modifications and computational instructions were given about a decade later by Thornthwaite and Mather (1955, 1957).

When expressed in today's notation, Thornthwaite's soil moisture budget is governed by

$$\partial w/\partial t = P - E - S \tag{1}$$

where $w$ is the moisture available in the root zone; and $P$, $E$ and $S$ are the rates of precipitation, evapotranspiration and surplus, respectively. Thornthwaite proposed that $E$ be made to depend on the rates of precipitation and potential evapotranspiration, as well as on the available soil moisture, in the following way:

$$E = \begin{cases} P + \beta(w, w^*)[E^0(T, h) - P], & P < E^0(T, h) \\ E^0(T, h), & P \geq E^0(T, h) \end{cases} \tag{2}$$

where $w^*$ is the soil moisture storage capacity, $E^0$ is potential evapotranspiration (evapotranspiration when the vegetation cover is not under any water stress), $T$ is the daily average surface air temperature, $h$ is the duration of daylight and $\beta$ is a function that relates $[(E - P)/(E^0 - P)]$ to $(w/w^*)$. As required by mass continuity, Thornthwaite considered $S$ to include both surface and subsurface run-off from the root zone and he let

$$S = \begin{cases} P - [E + (w^* - w)], & P > [E + (w^* - w)] \\ 0, & P \leq [E + (w^* - w)] \end{cases} \tag{3}$$

Elements of Thornthwaite's soil moisture budget have been modified many times, but equations (1), (2) and (3) continue to provide the guiding principles.

With the intention of producing a world water balance atlas, Thornthwaite and his associates at the C. W. Thornthwaite Laboratory of Climatology began, in 1947, to assemble the required precipitation and temperature records from stations all over the globe. During the years 1950–1957, when Thornthwaite served as the President of the Commission on Climatology of the World Meteorological Organization, the data acquisition effort became one of the Laboratory's major activities. The compilation was essentially complete by 1962, at which time Thornthwaite and his associates had collected usable monthly mean records from 14,765 stations; although, the stations had a very uneven spatial distribution and their lengths of record varied from several decades to only a few years.

Thornthwaite, Mather and their colleagues at the Laboratory subsequently used these data to obtain average monthly totals of $E^0$, $E$ and $S$, as well as end-of-the-month values of $w$ for each station. The station values of $E^0$, $E$ and $w$, together with mean monthly $P$, $S$ and water deficit $(E^0 - E)$, were published for 1069 African stations (Mather, 1962); 1660 Asian stations—excluding the U.S.S.R. (Mather, 1963a); 697 stations in the U.S.S.R. (Mather, 1963b); 532 stations in Australia, New Zealand and Oceania (Mather, 1963c); 1442 stations in Europe (Mather, 1964a); 1106 North American stations—excluding the United States (Mather, 1964b); 1228 stations in the United States (Mather, 1964c) and 831 stations in South America (Mather, 1965). For all the continents then, 8565 station water balances were published. The temperature records were not published.

The water balance atlas of the world was never completed, although small-scale maps ($1:5 \times 10^6$) of mean annual potential evapotranspiration ($\bar{E}^0$), surplus ($\bar{S}$) and deficit ($\bar{E}^0 - \bar{E}$) were published for the 'Red Sea' sector ($\simeq$25°E to 47°E and 14°N to 42°N) and for the adjacent 'Persian Gulf' sector ($\simeq$45°E to 70°E and 13°N to 38°N) (both in Thornthwaite *et al.*, 1958a) and for the 'Eastern North American' sector ($\simeq$65°W to 97°W and $\simeq$25°N to 55°N) (Thornthwaite *et al.*, 1958b). The data were also used by van Hylckama (1956) to estimate the total monthly water detention on the continents; and by the

Laboratory—under contract to the United States Army Corps of Engineers—to estimate soil tractionability for various regions of the world (C. W. Thornthwaite Associates, 1954).

Many years later, Strahler and Strahler (1978, Figure 10.11) made a small-scale ($1:1{\cdot}3\times10^8$) global map of $\bar{E}^0$ from the data tabulations of Mather (1962; 1963a,b,c; 1964a,b,c; 1965). Baumgartner and Reichel (1975, pp. 20–25 and Plates 5, 7, 10–14, 17–20) used the same data set to obtain maps of annual mean actual evapotranspiration, $\bar{E}$, for the continents. Wherever Baumgartner and Reichel had a measurement of mean annual river flow, they adjusted the evapotranspiration field over that river's drainage basin so that the area-averaged $\bar{E}$ would equal their own area-averaged $\bar{P}$ minus the measured river flow.

Recently, the precipitation and temperature data for 13,332 of the Laboratory's stations have been edited, augmented, magnetically encoded and published by Willmott *et al.* (1981).

## TERRESTRIAL WATER BUDGET

### *Background*

Inasmuch as the present study is guided by Thornthwaite's water budget principles and makes use of the station records that he assembled, it can be regarded as a continuation of Thornthwaite's global water budget work. It differs, however, from the earlier terrestrial water balances published by the Laboratory (Mather, 1962; 1963a,b,c; 1964a,b,c; 1965) in several respects:

1. The water balance calculations are made for 13,332 stations which have complete air temperature and precipitation records (Willmott *et al.*, 1981). Mather (1962; 1963a,b,c; 1964a,b,c; 1965) gave water balances for only 8565 of the 14,765 stations assembled by the Laboratory.
2. A snow-cover budget is included, in addition to the soil moisture budget. Taking the snow accumulation and snow-melt into account has only a minor influence on the Thornthwaite calculation of evapotranspiration, but it gives a more realistic time variation of the soil moisture store.
3. The evapotranspiration function $\beta(w, w^*)$, and storage capacity ($w^*$) have been changed to follow Mintz and Serafini (1984) rather than Mather (1962; 1963a,b,c; 1964a,b,c; 1965).
4. All of the monthly components of the station water balances have been interpolated (following Willmott *et al.*, 1985) to a 1° of latitude by 1° of longitude lattice, and both the station and gridded water balance fields are available in machine readable (magnetic tape) form.

A similar study of the terrestrial water balance has recently been made by Mintz and Serafini (1984) although they use other sources for precipitation (Jaeger, 1976; Spangler and Jenne, 1984) and, like Thornthwaite, they do not carry a separate budget for snow-cover.

### *Governing equations*

As indicated above, we evaluate separate budgets for the moisture stored in the soil ($w$) and for the water contained in the snow-cover ($w^s$). In the higher latitudes and elevations, these two water budgets are linked through snow-melt; therefore, we take their time rates of change, respectively, as

$$\partial w^s/\partial t = P^s - M \tag{4}$$

and

$$\partial w/\partial t = P^r + M - E - S \tag{5}$$

where $P^s$ is the snowfall rate (water equivalent), $M$ is the snow-melt rate (water equivalent), $P^r$ is the rainfall rate, $E$ is again the evapotranspiration rate and $S$ is again the surplus rate. When the snow-melt is taken into account, evapotranspiration (equation (2)) becomes

$$E = \begin{cases} P^r + M + \beta(w, w^*)[E^0(T, h) - P^r - M], & (P^r + M) < E^0(T, h) \\ E^0(T, h) & (P^r + M) \geq E^0(T, h) \end{cases} \tag{6}$$

where $\beta$ now relates $[(E-P^r-M)/(E^0-P^r-M)]$ to $(w/w^*)$, and surplus is

$$S=\begin{cases}P^r+M-[E+(w^*-w)], & (P^r+M)>[E+(w^*-w)]\\ 0, & (P^r+M)\leq[E+(w^*-w)]\end{cases} \tag{7}$$

Precipitation is either rain ($P^r$) *or* snow ($P^s$) according to

$$P=\begin{cases}P^r, & T\geq c\\ P^s, & T<c\end{cases} \tag{8}$$

where $c$ is a constant, index temperature (°C). Snow-melt is taken to be

$$M=\begin{cases}M(T,P^r), & w^s>0\\ 0, & w^s=0\end{cases} \tag{9}$$

which assumes that the snow-melt can be adequately estimated from the air temperature and the internal energy of an above-freezing rain.

The physical rationale for equation (9) is that vegetation which protrudes through the snow is heated by insolation. The heating is especially efficient in latitudes where the solar zenith angle is large. Beneath and adjacent to the canopy, net long-wave radiational transfer from the canopy melts the snow. The canopy also warms the air that blows through it and this warmed air can melt the snow by sensible heat transfer, even at some distance from the radiational influence of the canopy. Air temperature then is an index for both of these snow-melt processes. From studies made in north-eastern Quebec, for instance, FitzGibbon and Dunne (1983) show that sensible heat flux provides the major energy source for snow-melt when the canopy is sparse and net radiation is the dominant snow-melt energy source under more dense canopy. Once again, equation (9) also takes into account the snow-melt that results from above-freezing rain.

*Computational method*

*Potential evapotranspiration.* Following Thornthwaite (Wilm *et al.*, 1944; Thornthwaite, 1948), monthly unadjusted potential evapotranspiration is first taken as

$$E^{0\prime}(\text{mm/month})=\begin{cases}0, & T<0°\text{C}\\ 16(10T/I)^a, & 0\leq T<26{\cdot}5°\text{C}\\ -415{\cdot}85+32{\cdot}24T-0{\cdot}43T^2, & T\geq 26{\cdot}5°\text{C}\end{cases} \tag{10}$$

where $T$ is the mean monthly surface air temperature (°C),

$$I=\sum^{12}(T/5)^{1{\cdot}514} \tag{11}$$

and

$$a=6{\cdot}75\times10^{-7}I^3-7{\cdot}71\times10^{-5}I^2+1{\cdot}79\times10^{-2}I+0{\cdot}49 \tag{12}$$

To account for variable day and month lengths, $E^{0\prime}$ is adjusted to

$$E^0(\text{mm/month})=E^{0\prime}[(\theta/30)(h/12)] \tag{13}$$

where $\theta$ is the length of the month (in days) and $h$ is taken as the duration of daylight (in hours) on the fifteenth of the month.

Thornthwaite obtained the above relationship for $E^0=E^0(T,h)$ by regressing measured monthly surface air temperature and the duration of daylight with (1) measured monthly evapotranspiration from some well-watered grass-covered lysimeters in the eastern and central United States and (2) the difference between measured river run-off and monthly precipitation for a few well-watered drainage basins in the eastern United States. Thornthwaite was aware that the direct physical connection was between $E^0$ and net radiation, rather than $T$, but he believed it would be a long time before a suitable

number of radiation measurements would be available. In the meantime, he reasoned that surface air temperature could be used as a proxy for the surface radiation flux (Thornthwaite and Hare, 1965). Nearly 30 years after Thornthwaite specified $E^0$ (Priestley and Taylor, 1972; de Jong, 1973), and even today, adequate information about the surface radiation fluxes is not available.

Relatively recent evaluations of performance document the collinearity between Thornthwaite-calculated and lysimeter-derived estimates of monthly $E^0$ as well as systematic differences or bias (Pelton *et al.*, 1960; McGuinness and Bordne, 1971; Jensen, 1973). Jensen (1973), for example, compared model-predicted $E^0$'s with monthly lysimeter estimates drawn from 10 sites and he observed a correlation between Thornthwaite- and lysimeter-derived $E^0$'s of 0·81. He also observed, as did McGuinness and Bordne (1971), that the Thornthwaite values were consistently low. Jensen (1973) reports an overall monthly root mean square error (RMSE) of 1·84 mm day$^{-1}$. If the lysimeter-derived values are correct, this error seems large, but we also know that lysimeter measurements can systematically exceed the evapotranspiration from surrounding grass-covered fields (Mustonen and McGuinness, 1968). It may be, therefore, that Thornthwaite's values are closer to actual, regional $E^0$ than Jensen's RMSE suggests. In fact, if one attributes the systematic (linear) difference between Thornthwaite's and the lysimeter estimates of $E^0$ to lysimeter bias, the RMSE expectation reduces to 0·92 mm day$^{-1}$ (Willmott, 1984) which is comparable to the RMSEs of several well-known radiation-based and combination methods (Jensen, 1973). These findings indicate that the Thornthwaite calculations provide more precise and probably more accurate estimates of monthly $E^0$ than is often assumed (Willmott, 1984).

*Water budget.* Water storage is partitioned between snow-cover and soil moisture stores, and $\partial w^s/\partial t$ and $\partial w/\partial t$ are evaluated on a quasi-daily basis, i.e. 30 times per month (Willmott, 1977). Calculation of the snow and soil water stores begins with the water contained in the snow-cover at the conclusion of a day. The subscript $d$ is used when the variable changes from day to day, whereas the subscript $D$ indicates daily values that are constant over the month.

Snow-cover water equivalent (in mm), at the end of day $d$, is

$$w_d^s = w_{d-1}^s + P_D^s - M_d \tag{14}$$

where $w_{d-1}^s$ is the water contained in the snow-cover at the end of the previous day $(d-1)$, $P_D^s$ is the cumulative snowfall over day $D$ and $M_d$ is the snow-melt during day $d$. The calculations are made with $P_D^s = P^s/30$ and $P_D^r = P^r/30$, where $P_D^r$ is the daily rainfall, and

$$P(\text{mm/month}) = \begin{cases} P^r, & T \geq -1°\text{C} \\ P^s, & T < -1°\text{C} \end{cases} \tag{15}$$

following Thornthwaite and Mather (1955). Daily snow-melt (mm/day) is taken as

$$M_d = 2{\cdot}63 + 2{\cdot}55T_D + 0{\cdot}0912T_D P_D^r \tag{16}$$

where $T_D = T$ and $M_d$ is constrained so that $0 \leq M_d \leq (w_{d-1}^s + P_D^s)$. Comparisons between the equation (16) and the data from which it was derived—representing three dissimilar drainage basins and 113 daily observations (Anderson, 1973; Pysklywec *et al.*, 1968; Storr, 1978)—suggest a moderately good fit, i.e. RMSE = 6·62 mm day$^{-1}$ and $r^2 = 0{\cdot}59$.

Evaporative demand from the surface or soil water surplus (in mm/day) is

$$D_d = M_d + P_D^r - E_D^0 \tag{17}$$

where $E_D^0 = E^0/30$. When $D_d$ is negative, it represents a demand; when positive, it constitutes recharge, or a surplus when the soil is at storage capacity. Following Mintz and Serafini (1984) (based on Nappo (1975) and Davies and Allen (1973)), the evapotranspiration function is

$$\beta_d = \begin{cases} 1 - \exp(-6{\cdot}68 w_{d-1}/w^*), & D_d < 0 \\ 1, & D_d \geq 0 \end{cases} \tag{18}$$

where $w_{d-1}$ is the soil moisture at the beginning of day $d$. Soil moisture at the end of day $d$ (in mm) then becomes

$$w_d = w_{d-1} + \beta_d D_d \tag{19}$$

When ($w_d > w^*$), the difference is retained as the surplus ($S_d$) for day $d$, and $w_d$ is set equal to $w^*$. It should be noted (see equation (6)) that $M_d$ and $P_D^r$ are assumed to evaporate at the maximum rate ($\beta_d = 1$), *after* which, if $D_d$ is negative, soil moisture is evapotranspired according to the reduced potential, $(E_D^0 - M_d - P_D^r)$, at the $\beta_d$ rate. The gain or loss of soil moisture for the month ($\Delta w$) then is the difference between $w_{30}$ and its magnitude at the end of the previous month. Monthly evapotranspiration ($E$) is finally obtained as the residual from

$$E(\text{mm/month}) = P^r + \sum^{30} M_d - \Delta w - \sum^{30} S_d \tag{20}$$

*Balancing the water budget.* When the monthly average air temperature and precipitation time series are stationary, an annual water *balance* can be assumed and each $w_d$, and $w_d^s$ can be iteratively adjusted toward climatic equilibrium. Our solution to this problem begins with the assignment of an initial soil moisture ($w_1 = w^*$) and snow-cover water equivalent ($w_1^s = P_1^s$) for 1 January. The above-described water budget is then integrated forward in time, over the year, until $w_1$ and $w_1^s$ are obtained for the next 1 January. The calculations are then repeated with the new values of $w_1$ and $w_1^s$ until they produce negligible changes in $w_1$ *and* $w_1^s$ ($\leq$1 mm) between two adjacent years. The most recently calculated mid-monthly estimates of $w_d$ and $w_d^s$ are taken as the climatically representative monthly soil moistures and snow-covers, respectively.

At some high-latitude stations (principally in Antarctica), the water budget does not balance because $\int_{\text{year}} (P^s - M)\, dt > 0$. Where this occurs, we calculate the annual rate of accumulation instead of the annual mean of $w^s$.

## TERRESTRIAL SEASONAL WATER CYCLE

Using the monthly air temperature and precipitation data described above, monthly water budgets were computed for the 13,332 stations (Figure 1). The soil moisture capacity ($w^*$) was taken as 150 mm, following Mintz and Serafini (1984). At each station, mid-monthly snow-cover water equivalent ($w_{15}^s$), mid-monthly soil moisture ($w_{15}$) and monthly evapotranspiration ($E$) were calculated.

As an example, we show the monthly water budget for Schefferville, Quebec (54°49′N, 66°41′W) (Figure 2). Another budget is also shown (Figure 2) that follows the governing equations given by Thornthwaite (primed symbols, *i.e.* $w'_{15}$, $E'$ and $S'$). It treats all precipitation as rainfall. Thornthwaite's rationale was that almost no evapotranspiration takes place while the snow is accumulating on the surface; consequently, it does not matter whether one lets the water enter the soil during the snow accumulation months or during the snow-melt months. The Schefferville example supports this. In both budgets, $\beta$ is nearly 1·0 in the summer months and the two evapotranspirations, $E$ and $E'$, are almost the same. This, in turn, makes the annual mean surpluses, $\bar{S}$ and $\bar{S}'$, very nearly the same although the monthly surpluses are not.

Values of $w_{15}^s$, $w_{15}$ and $E$ then were spatially interpolated to the nodes of a 1° of latitude by 1° of longitude grid. The interpolation was made using the spherically based method described by Willmott *et al.* (1985), except that the number of nearby data points (stations) which influenced a grid point was held constant at 10. To preserve map clarity, we show the interpolated fields only for a subset of the 1° × 1° lattice; that is, at the nodes of a 4° of latitude by 5° of longitude grid.

Each variable at each 4° × 5° node then was decomposed harmonically into an annual mean ($\bar{w}_{15}^s$, $\bar{w}_{15}$ and $\bar{E}$) and the first two annual harmonics ($\hat{w}_{15}^s(1)$, $\hat{w}_{15}^s(2)$; $\hat{w}_{15}(1)$, $\hat{w}_{15}(2)$; $\hat{E}(1)$, $\hat{E}(2)$). This decomposition is illustrated for the Schefferville station (Figure 3).

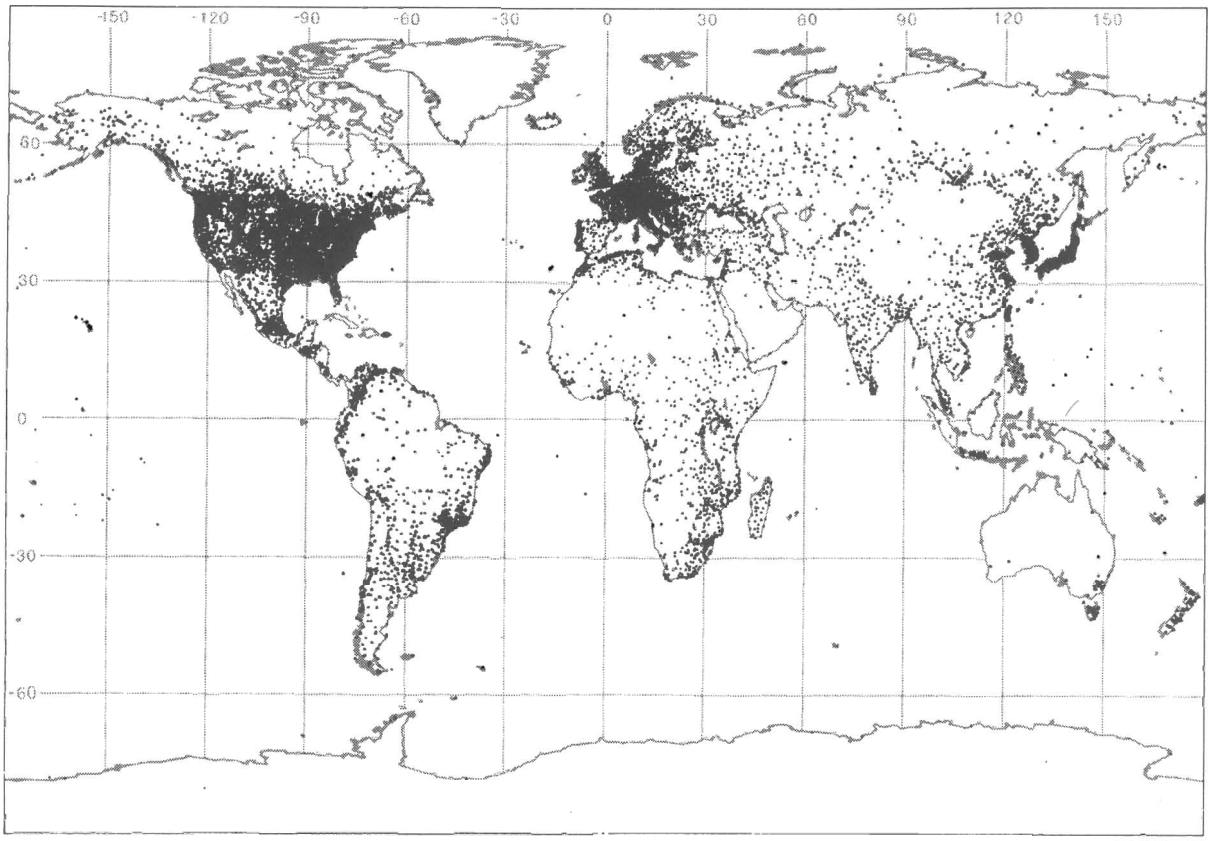


Figure 1. Distribution of the stations at which monthly water balances were computed

*Snow-cover*

Mean annual snow-cover ($\bar{w}_{15}^{s}$) (given as an equivalent depth of the water) generally increases poleward, but with several departures (Figure 4(a)). For example, a maximum occurs at about 55°N near the east coast of North America, owing to the relatively high winter precipitation rates. Over the Rocky, Pyrenees, Caucasus and Ural mountains, one sees the orographic effect on precipitation and temperature. Except for Antarctica, we show very little snow-cover in the southern hemisphere; principally because our 4° × 5° grid is too coarse to capture small areas of snow-cover, such as in the mountains of New Zealand and the southern Andes. Over Antarctica, $\int_{\text{year}} (P^{s} - M)\, dt > 0$ which means there is not an equilibrium for the region but rather an annual accumulation. Even though one expects $\int_{\text{year}} (P^{s} - M)\, dt > 0$ over the interior of Greenland, no accumulation is shown because we have no interior station (Figures 1 and 4(a)).

The standard deviation of $w_{15}^{s}(\hat{\sigma}^{s})$ is roughly colinear with $\bar{w}_{15}^{s}$, since $w_{15}^{s}$ is bounded on the low end by zero (Figure 4(b)). Along the east coast of North America, for example, the seasonal variance increases with latitude to approximately 55°N and then $\hat{\sigma}^{s}$ begins to decrease with the latitudinal decrease in winter precipitation and the decrease in the length of the melt season. Mountainous regions of the northern hemisphere also show large seasonal variances (Figure 4(b)).

Over all of the continents, the variation not accounted for by the first two harmonics, $[(1 - r^{2})\hat{\sigma}^{s2}]^{0.5}$, is no more than about 10 mm. The residuals associated with our two-harmonic representations of $w_{15}^{s}$, $w_{15}$, and $E$ are illustrated for Schefferville, Quebec (Figure 3).

Phase angles (times of the maxima) of the first snow-cover harmonics represent the end of an

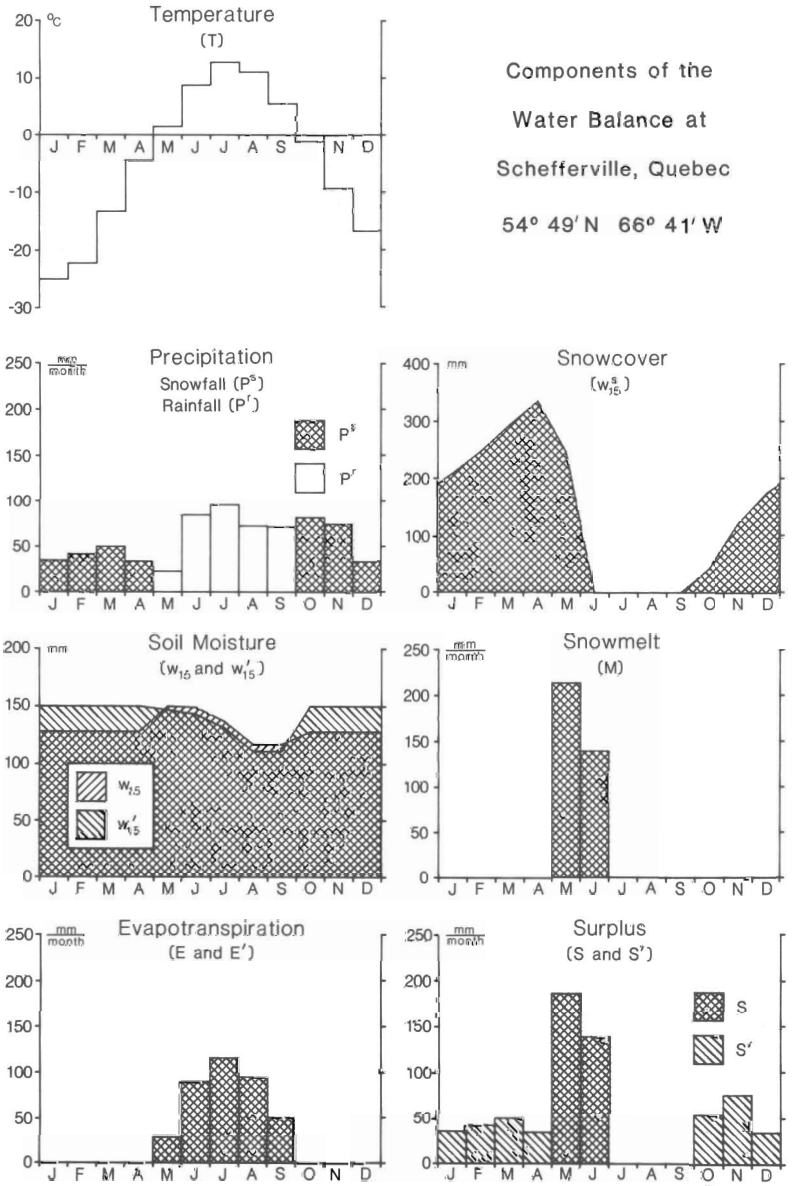


Figure 2. Average annual cycles of the components of the terrestrial water balance at Schefferville, Quebec. Primes are used to indicate the water balance components (*i.e.* $w'_{15}$, $E'$ and $S'$) calculated from Thornthwaite's original method, that is without our snow-cover correction

accumulation season and the onset of melt (Figure 4(c)). In the northern hemisphere, they show a clockwise shift—from January and February near the equatorward extent of the seasonal snow-cover to March and April in the higher latitudes. There is also a clockwise rotation of the phases from west to east across the United States and southern Canada. In mountainous areas (e.g. the Sierra Nevada, the Pyrenees and the Himalayas), the phases are delayed until March or April because of the increased depth of the snow-cover and the longer accumulation season. The largest amplitudes associated with the first harmonic occur in the latitude band where it is cold enough for the precipitation to be in the form of snow but not so cold that the amount of snowfall is small. Similar patterns appear in Antarctica but they are four or five months out of phase (Figure 4(c)).

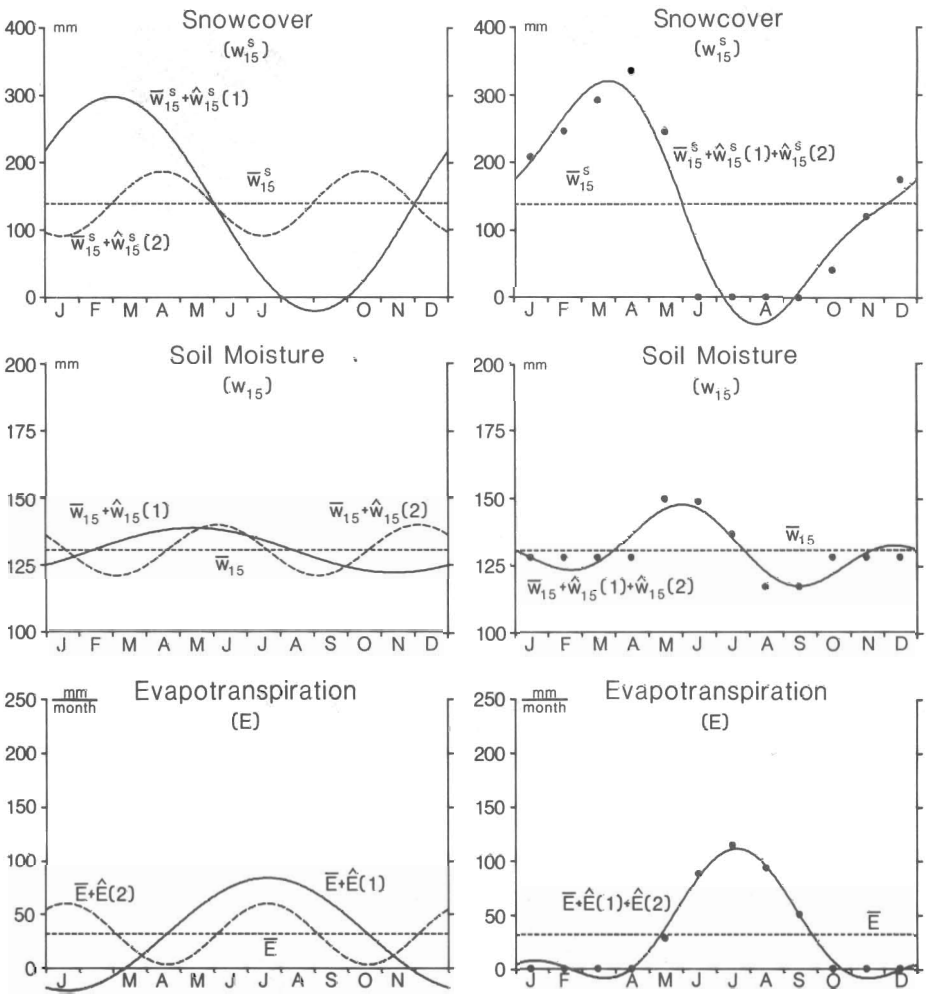


Figure 3. Harmonic representation of the seasonal snow-cover ($w_{15}^s$), soil moisture ($w_{15}$) and evapotranspiration ($E$) cycles at Schefferville, Quebec. The water-balance estimated values of $w_{15}^s$, $w_{15}$ and $E$ are the solid circles

Near the equatorward limit of the snow-cover, phase shifts of the second snow-cover harmonic (Figure 4(d)) are approximately the same as the phase angles of the first harmonic. Angular differences between the phases of the two harmonics, however, increase poleward with a clockwise rotation to a maximum difference of about three months. Second harmonic amplitudes increase with distance from the equator. When comparing the amplitudes of the first and second harmonics, note that the two representations (Figures 4(c) and 4(d)) differ by a factor of five.

*Soil moisture*

Annual mean soil moisture is more spatially variable than average snow-cover (Figure 5(a)). Eastern North America, south-east Asia, equatorial South America and equatorial Africa are regions where, over large areas, $\bar{w}_{15}$ exceeds 125 mm. Narrow zones of high soil moisture are also found along the north-west coast of North America and the south-west coast of South America. The soil is relatively dry in a broad band that extends southward from the western plains of Canada into the south-western United States and Mexico. A similar, but more narrow, band extends from Peru across the Andes, and into Patagonia.

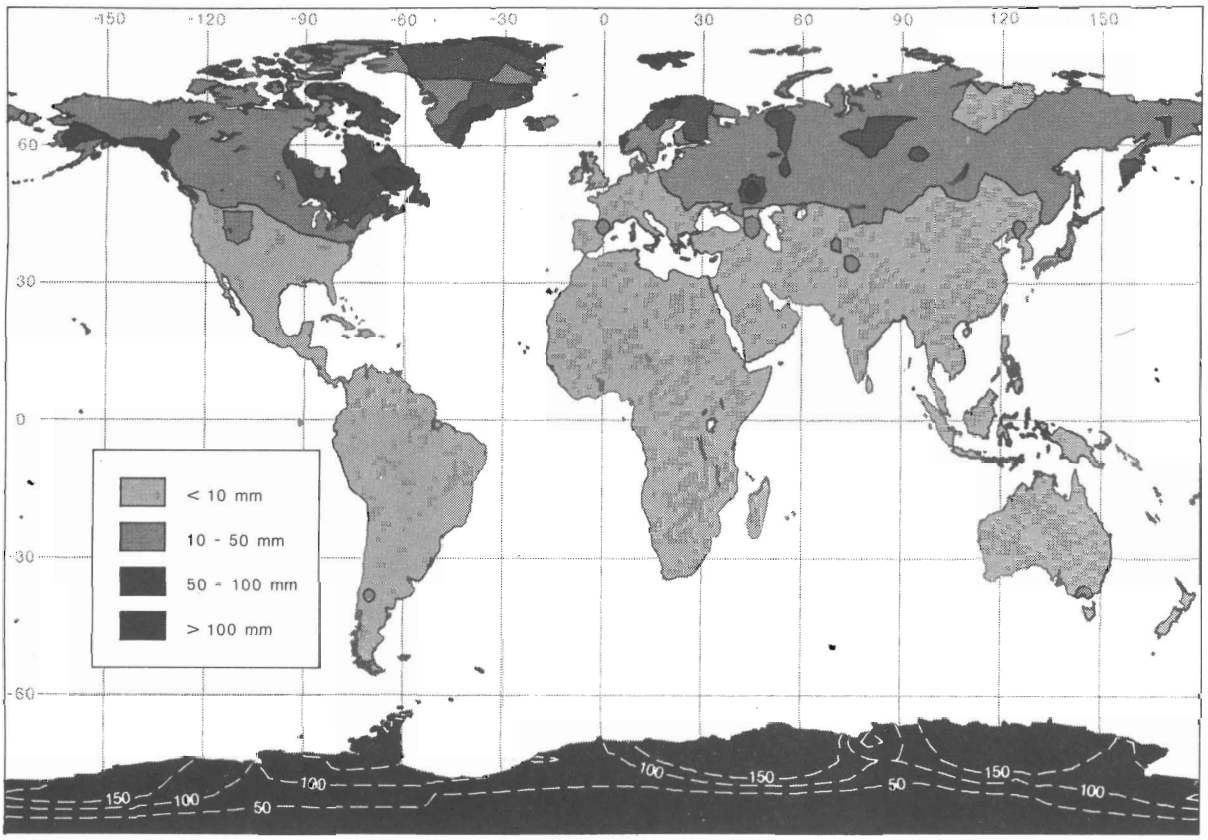


Figure 4(a). Annual mean snow-cover depth (mm equivalent water). Over Antarctica, the spatial distribution of $\int_{\text{year}} (P^s - M)\, dt$ (mm equivalent water/year) is depicted by dashed isolines

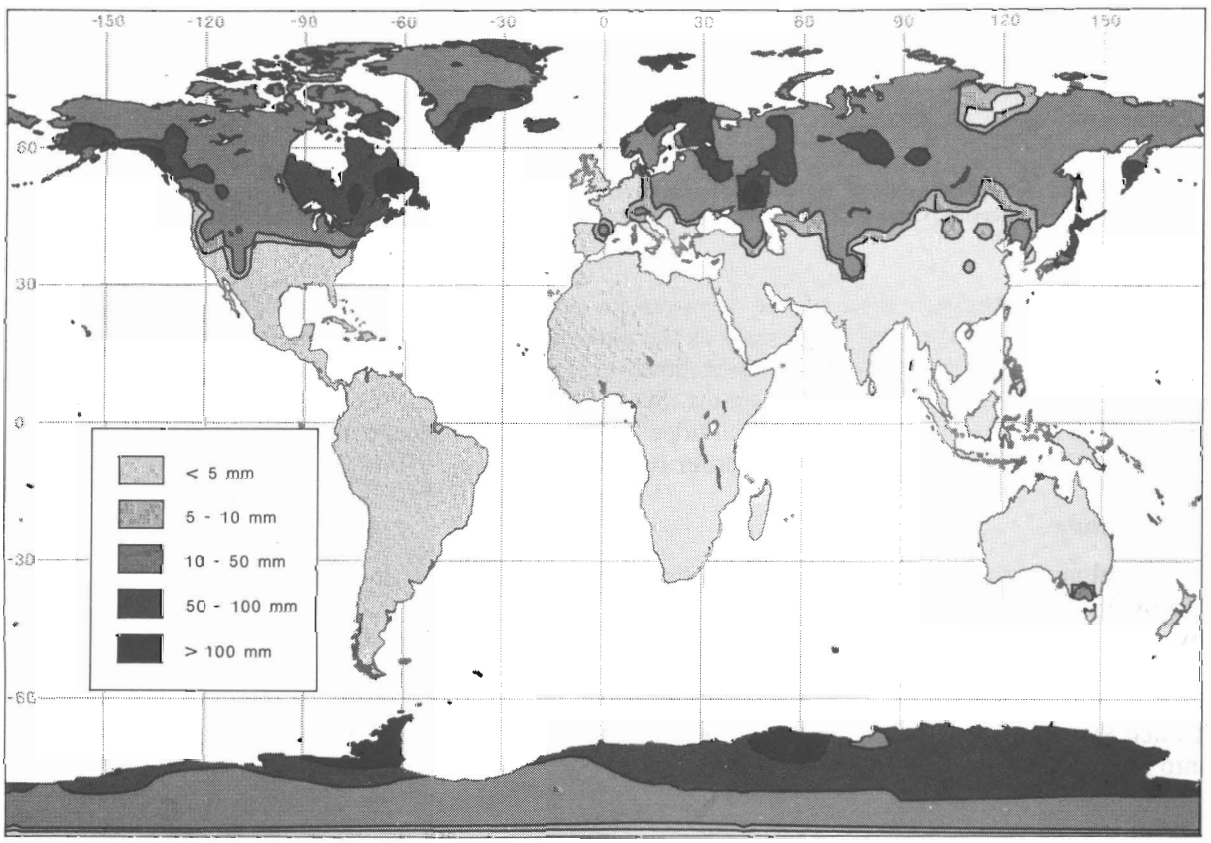


Figure 4(b). Standard deviations of mid-monthly snow-cover depth (mm equivalent water).

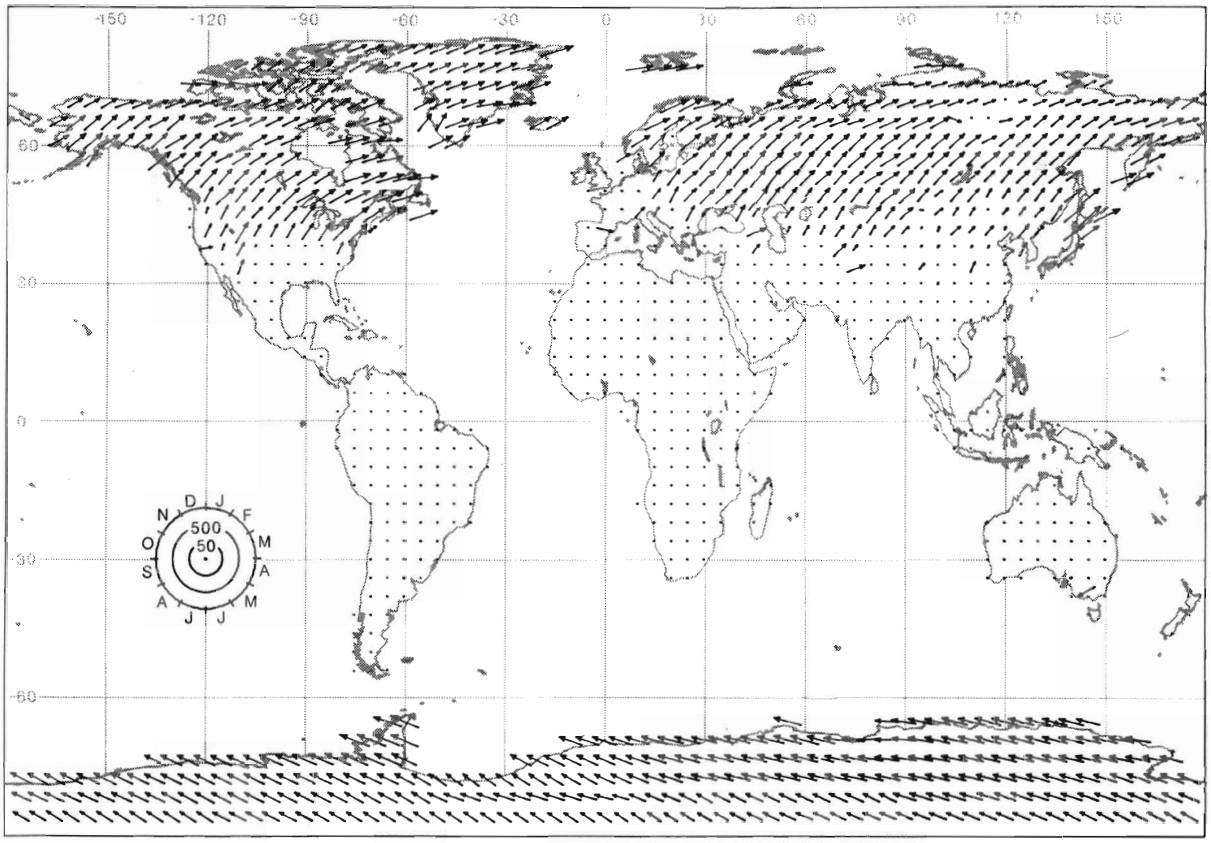


Figure 4(c). First harmonic of mid-monthly snow-cover depth (mm equivalent water). Amplitude is proportional to the length of an arrow (measured from the centre of the scale/dial) while the phase angle is given by its direction in months (see the edge of the scale/dial)

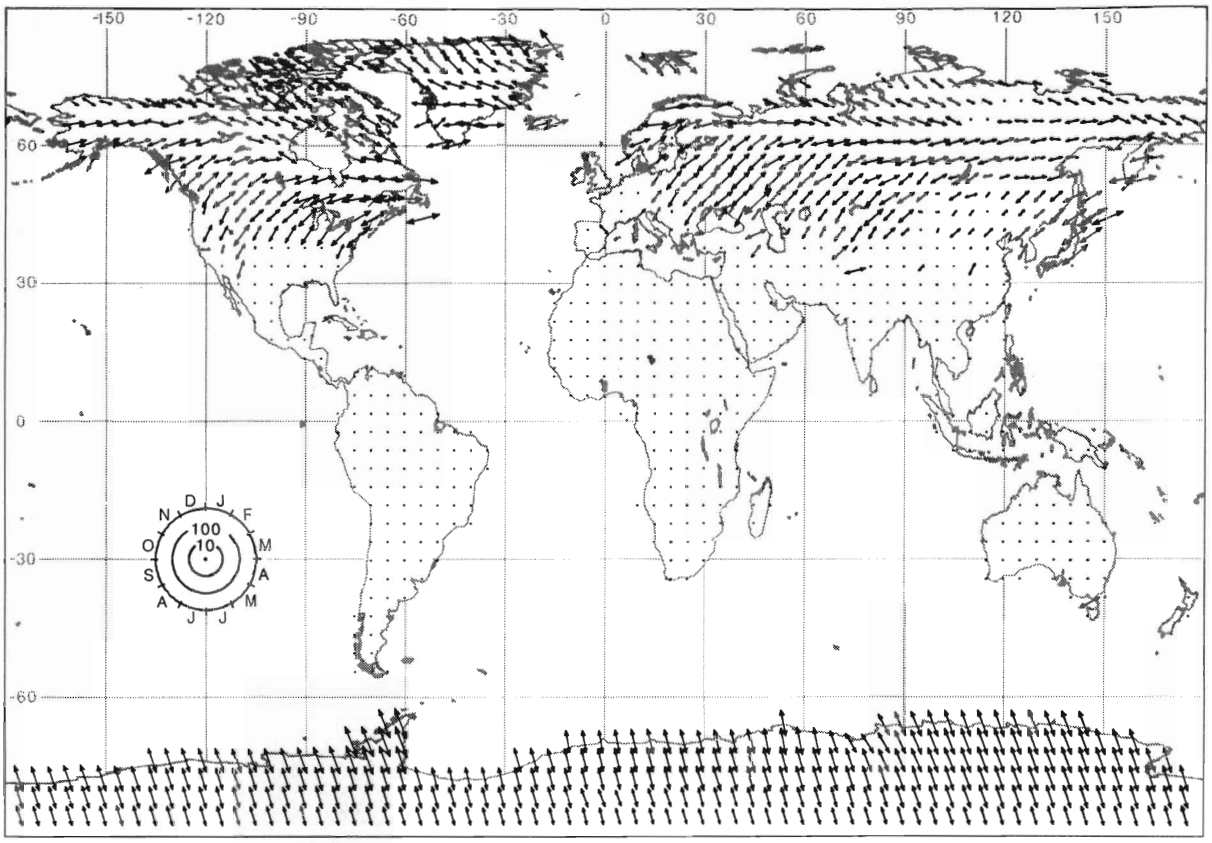


Figure 4(d). Second harmonic of mid-monthly snow-cover depth (mm equivalent water). Amplitude is proportional to the length of an arrow and the times of the maxima (phase shift) are indicated by its supplementary directions. Note that the amplitude scale differs from that of the first harmonic by a factor of five

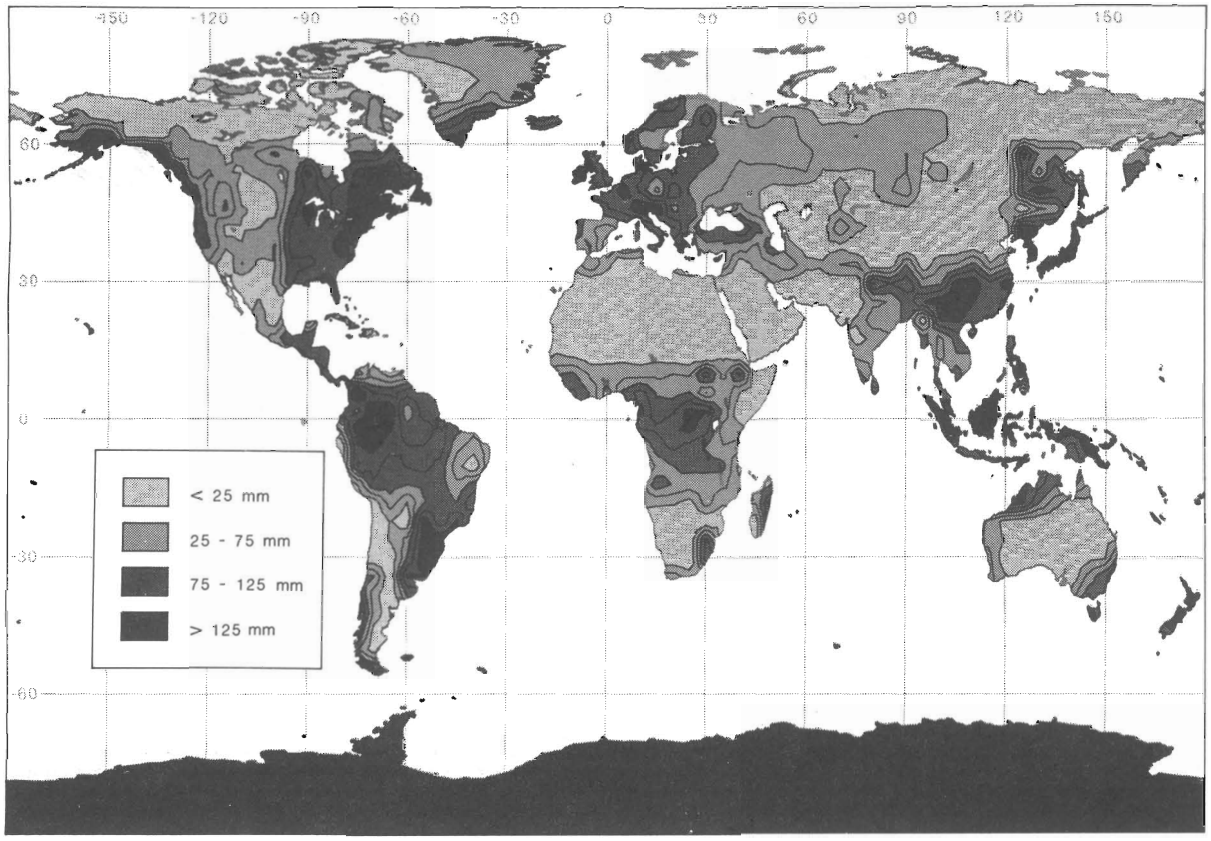


Figure 5(a). Annual mean soil moisture (mm). Intermediate isolines of 50 mm and 100 mm are given within the second and third categories, respectively, to improve the spatial resolution

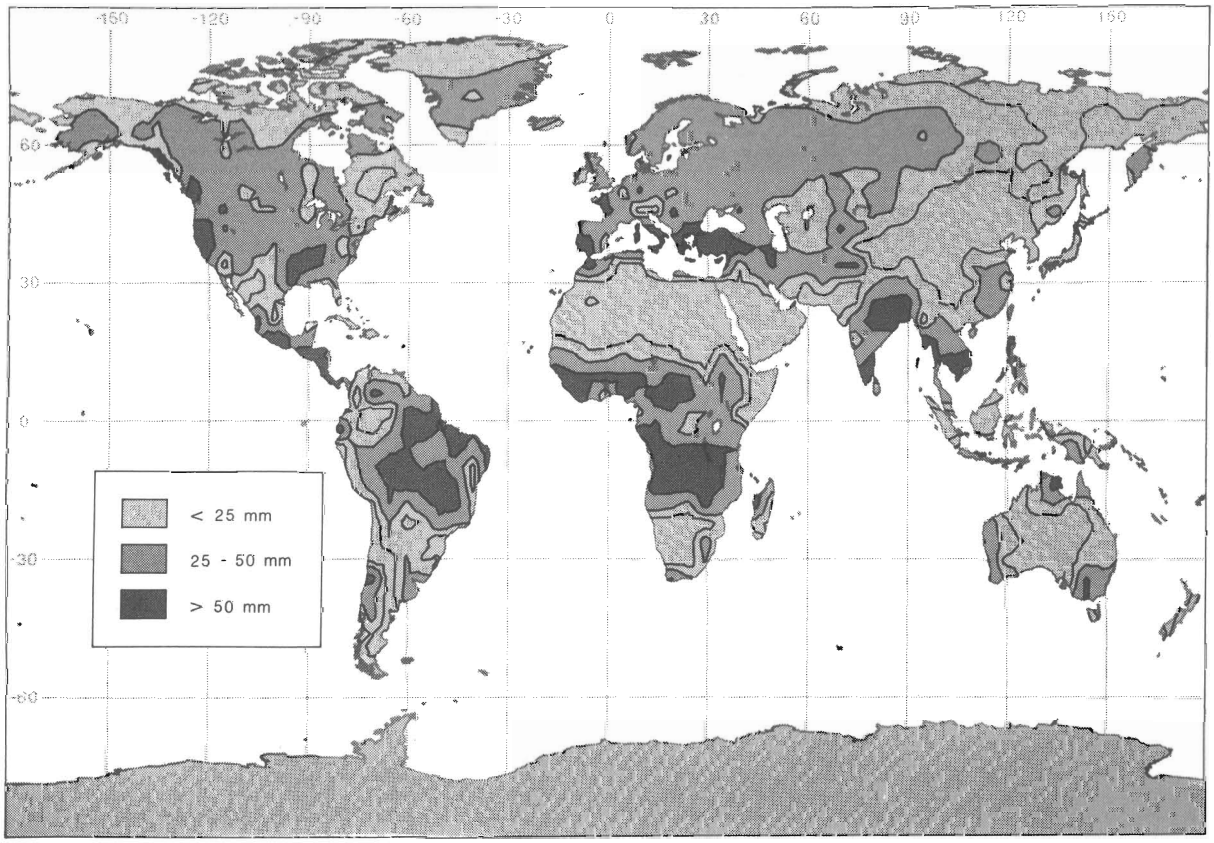


Figure 5(b). Standard deviations of mid-monthly soil moisture (mm). The 10 mm intermediate isoline is given within the first category to improve the spatial resolution

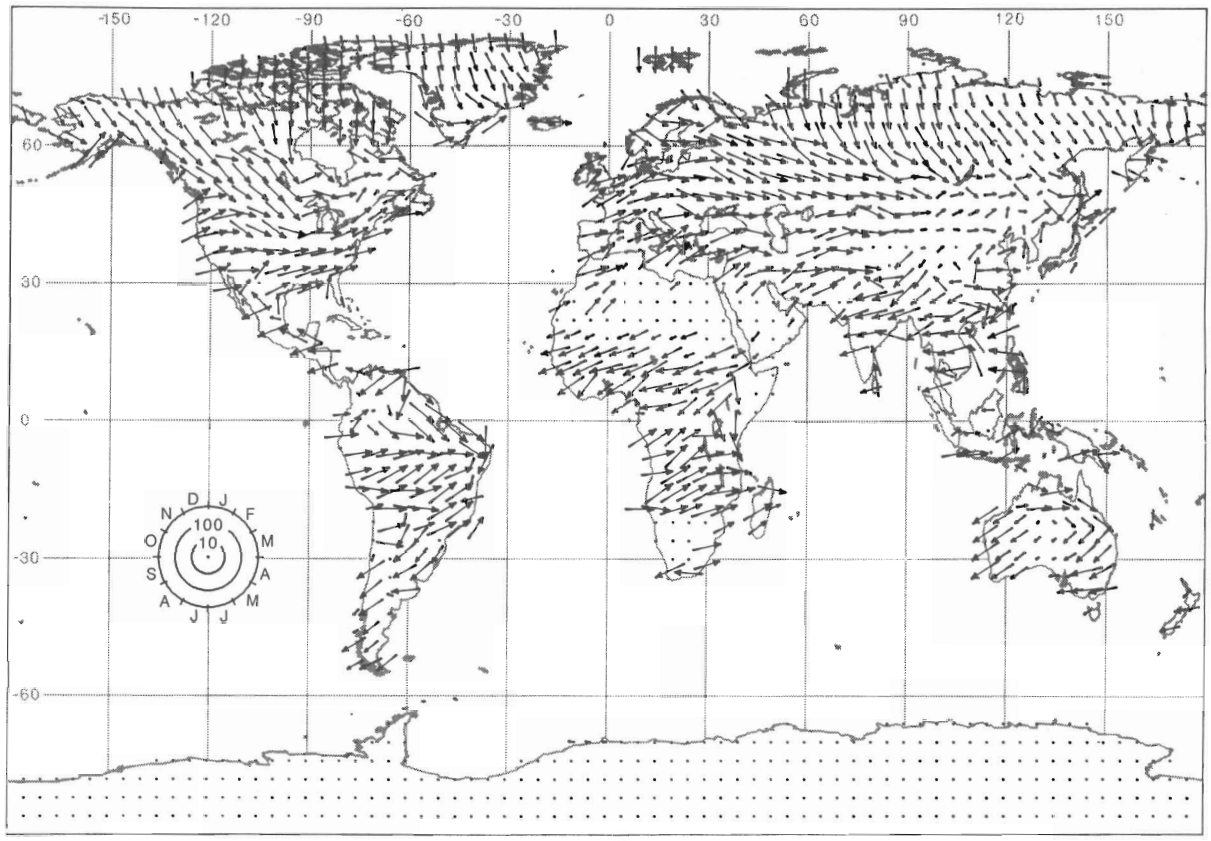


Figure 5(c). First harmonic of mid-monthly soil moisture (mm)

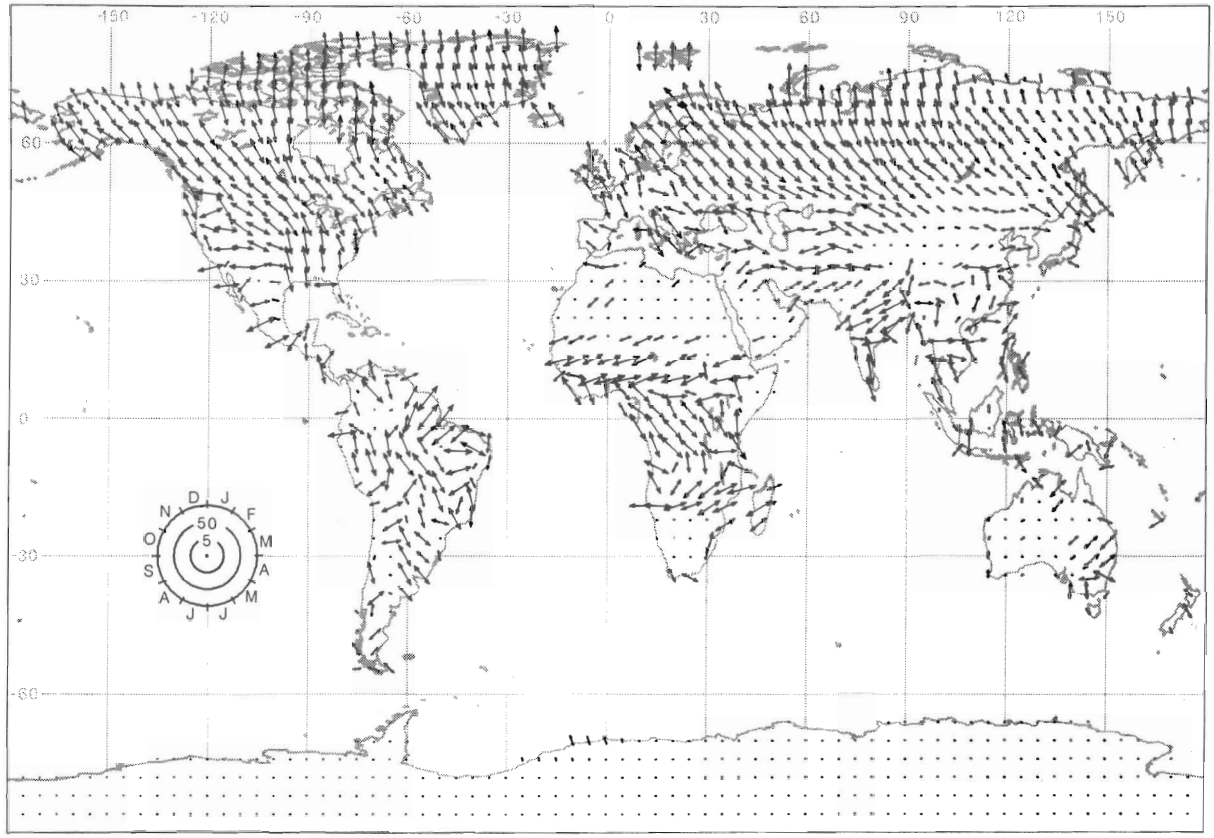


Figure 5(d). Second harmonic of mid-monthly soil moisture (mm). Note that the amplitude scale differs from that of the first harmonic by a factor of two

Within Europe too, average annual soil moisture is spatially variable, although few areas can be classed as dry (Figure 5(a)). From eastern Europe and continuing into central and western Asia, annual soil moisture decreases and the soil is very dry over much of north and central Asia. Only along the east coast of Asia, and in south-east Asia, are the levels of soil moisture high (>125 mm).

Within Africa, the dry extremes are the subtropical Saharan and circum-Sahara regions which together span most of northern Africa. South of the Sahara, over much of tropical Africa including the Ivory Coast, $\bar{w}_{15}$ is >75 mm. In south-western Africa, e.g. the Kalahari region, $\bar{w}_{15}$ is less than 25 mm.

Australia has dry soil ($\bar{w}_{15} < 25$) over most of its interior as well as along its east coast (Figure 5(a)). Only narrow bands of soil along the northern, western and south-eastern coastal regions are moist.

In general, the largest standard deviations of soil moisture fall in transition regions between large and small values of $\bar{w}_{15}$ (Figure 5(b)). Brazil, subtropical Africa, the Mediterranean region, the south-west coast of the United States and Monsoon Asia, for instance, display seasonal standard deviations in mid-monthly soil moisture greater than 50 mm.

When the soil moisture variance is harmonically decomposed, the first two harmonics again were sufficient to explain most of the variance contained in the annual soil moisture cycle (e.g. Figure 3). The variation left unaccounted for by the first two harmonics is generally less than 10 mm.

From the middle to the high latitudes of the northern hemisphere, there is a general clockwise rotation of the phases with increasing latitude (Figures 5(c) and 5(d)). Over mid-latitude North America and Eurasia, the soil water maximum is in March or April, and over northern North America and northern Eurasia, it is in May or June. This shows the increasing time lag in seasonal snow-melt as the latitude increases. Mountain and inland regions also have larger delays in the time of maximum soil moisture, relative to other regions in the same latitude, and this is apparent in the northern Rocky Mountains and the northern Great Plains. In the high latitudes, the effect of the late spring-time snow-melt is reinforced by the continuation of low spring-time potential evapotranspiration rates after the snow has gone.

Equatorward of the seasonal snow-cover, the time of the soil moisture maxima will not depend on snow-melt (Figure 5(c)). There, the maxima are at the ends of the periods during which precipitation exceeds evapotranspiration. Thus, in northern South America, the Sahel of Africa, India and south-east Asia, where the source of the soil moisture is the migrating belt of intertropical convergence rain, the maxima in the first annual harmonic of the soil moisture is August–September; in Argentina, south-central Africa and Indonesia it is February–March. In the Mediterranean region and south-western United States, the time of maximum soil moisture is also February–March, when the winter rains end.

In the higher latitudes of the northern hemisphere, the second harmonic of the soil moisture has about the same phase as the first harmonic (Figure 5(d)). This again shows the dominance of the snow-melt. In the middle latitudes of the northern hemisphere, however, the phase of the second harmonic is rotated clockwise with respect to the first harmonic. This represents a delay in the depletion of the soil moisture because the potential evapotranspiration is smaller in the spring than in the autumn.

*Evapotranspiration*

Where there is sufficient soil moisture, the evapotranspiration follows the potential evapotranspiration, which covaries with air temperature. For this reason, there is a general decrease of annual mean evapotranspiration ($\bar{E}$) with latitude (Figure 6(a)); upon this is superimposed the variation caused by soil moisture deficits.

Annual mean evapotranspiration is about 100 mm/month near the equator and 25 mm/month in the polar regions. Over the subtropical west coasts and across the Sahara, Arabia and central Asia, $\bar{E}$ is 25 mm/month or less.

The standard deviation of the monthly evapotranspiration (Figure 6(b)) is comparable in magnitude to the annual mean, wherever the annual mean is small. This is true in the high latitudes, where the available energy for evapotranspiration changes by a large amount during the year and also in those low latitude regions where the soil moisture has a large annual variation.

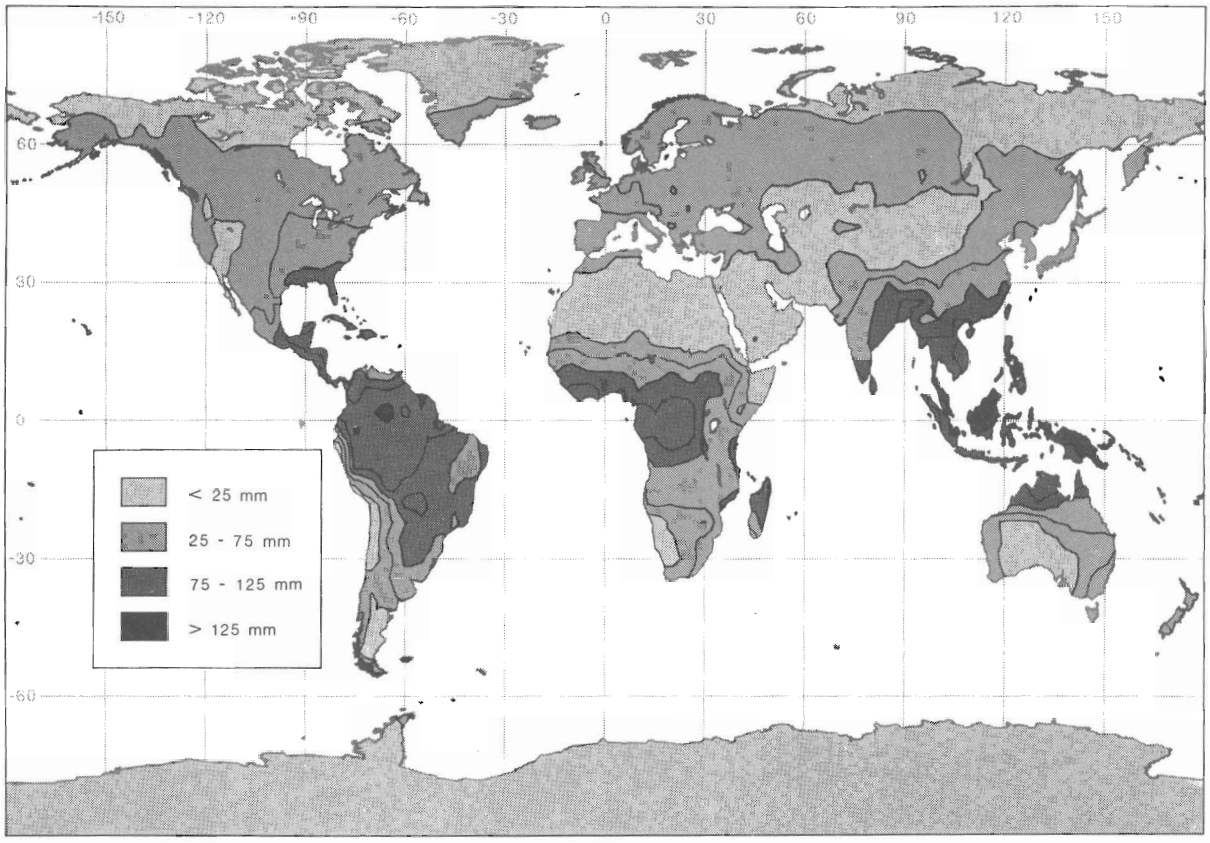


Figure 6(a). Annual mean evapotranspiration rate (mm/month). Intermediate isolines of 50 mm/month and 100 mm/month are given within the second and third categories, respectively

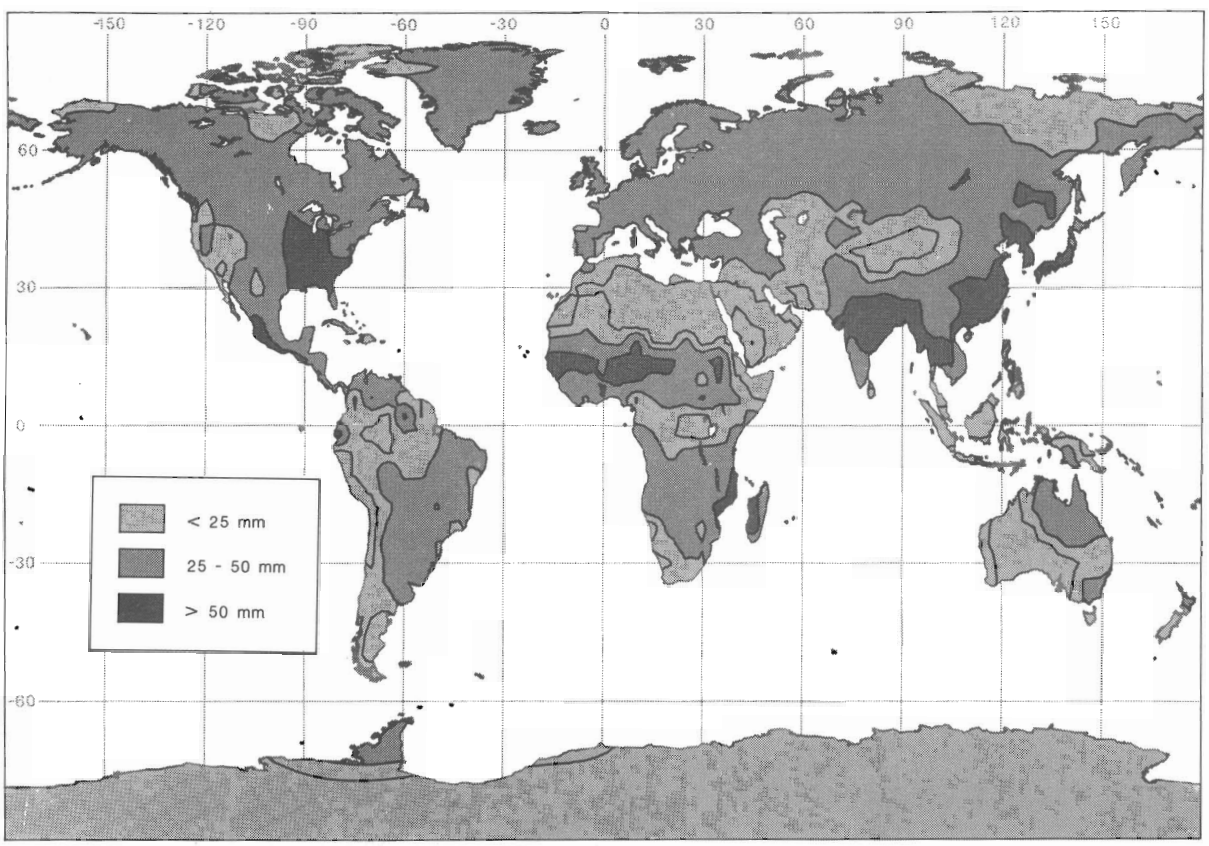


Figure 6(b). Standard deviations of monthly evapotranspiration (mm/month). The 10 mm/month intermediate isoline is given within the first category

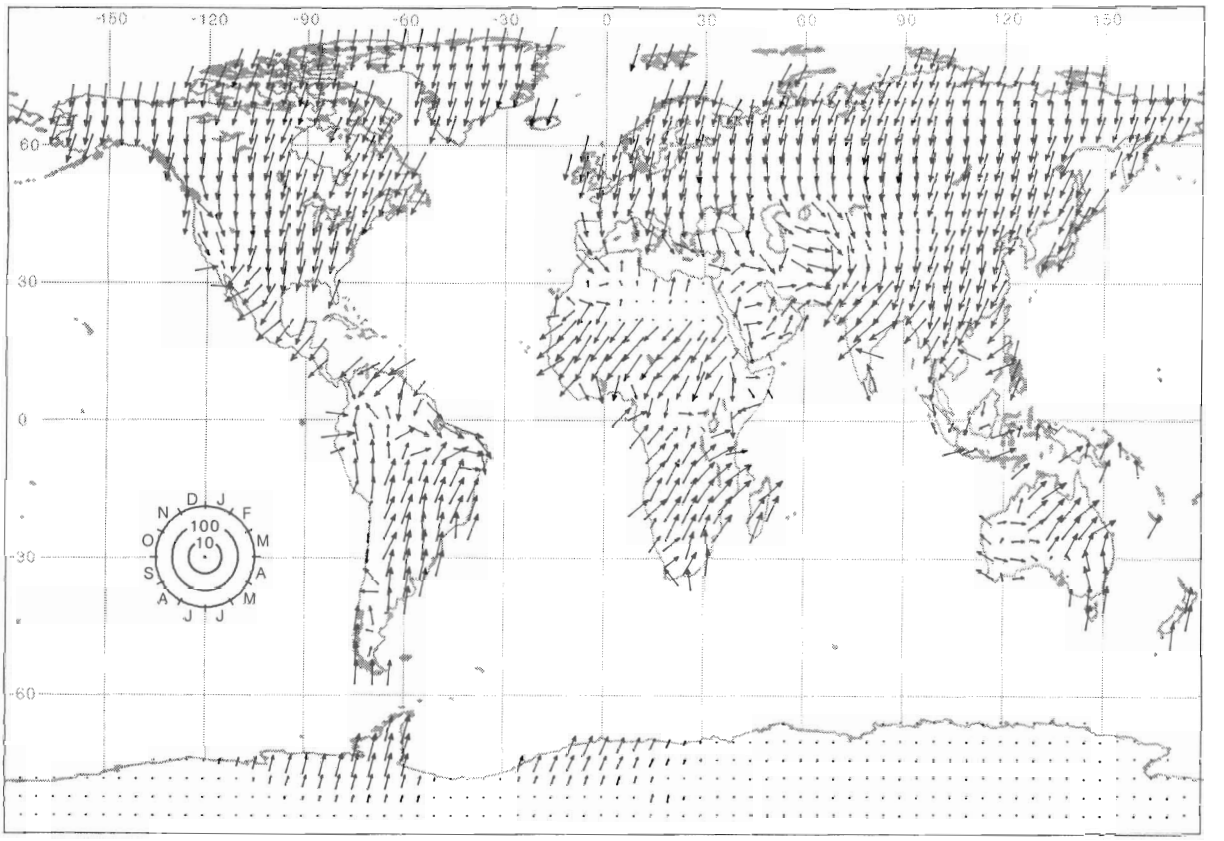


Figure 6(c). First harmonic of average monthly evapotranspiration (mm/month)

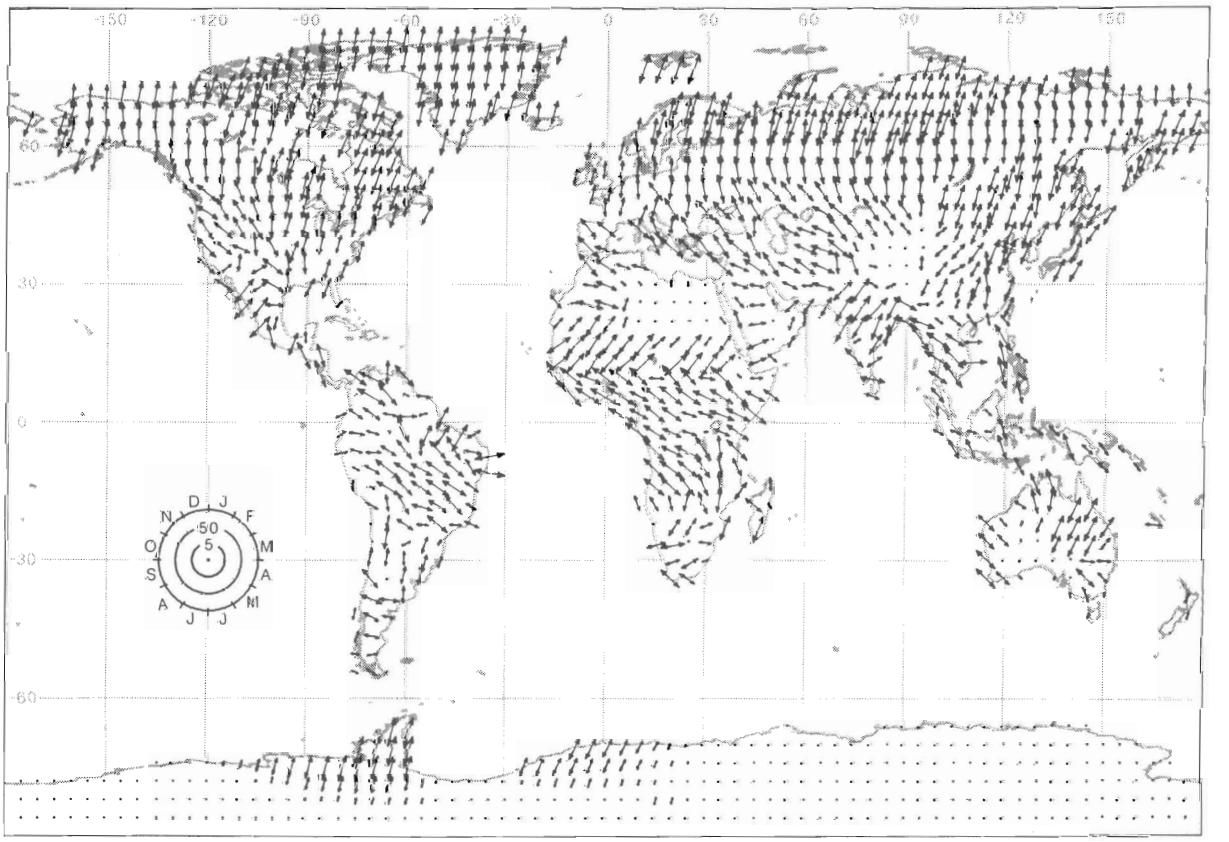


Figure 6(d). Second harmonic of average monthly evapotranspiration (mm/month). Note that the amplitude scale differs from that of the first harmonic by a factor of two

Most of the seasonal variation in evapotranspiration is accounted for by the first two annual harmonics (Figures 3, 6(c) and 6(d)). The second harmonic explains about half as much variance as the first and together they account for all but about 5 to 10 mm/month of the total variance. In the high and middle latitudes, the phase of the first harmonic coincides with the time of potential evapotranspiration (temperature) maximum: July in the northern hemisphere and January in the southern hemisphere. In the high latitudes, therefore, the evapotranspiration phase coincides with the soil moisture phase. In the middle latitudes, however, it is about three months later than the phase of the soil moisture maximum. Within the tropics, where there is no large seasonal potential evapotranspiration change, the evapotranspiration maximum occurs near the time of the soil moisture maximum. In the northern hemisphere tropics (Mexico, Central America, Africa and south-east Asia), this is in August or September.

The phase of the second annual harmonic of evapotranspiration is almost everywhere similar to that of soil moisture (Figures 5(d) and 6(d)).

## CONCLUDING REMARKS

Using monthly air temperature and precipitation data for the world and an empirically-based water budget algorithm, the large-scale spatial and seasonal variations of terrestrial snow-cover, soil moisture and evapotranspiration have been estimated. Of the three fields, snow-cover shows the greatest spatial and temporal regularity, particularly in the higher latitudes of the northern hemisphere. Terrestrial soil moisture is much more temporally and spatially variable than snow-cover. The magnitude of the seasonal snow water store, none the less, can be as large as or larger than the soil moisture store. Evapotranspiration varies less than soil moisture but more than snow-cover. This is principally because evapotranspiration is relatively insensitive to the changes in soil moisture until the soil moisture falls to very low values.

### ACKNOWLEDGEMENTS

Financial support from the Laboratory for Atmospheres at NASA's Goddard Space Flight Center in Greenbelt, Maryland (NASA Grant number NAG 5-107) is most gratefully acknowledged. The helpful comments of J. R. Mather and J. Shukla as well as the cartographic and technical assistance of H. J. Macintire and J. Bartoshesky also are gratefully appreciated.

## REFERENCES

Anderson, E. A. 1973. *National Weather Service River Forecast System—Snow Accumulation and Ablation Model*, NWS, USDOC (NOAA Tech. Memo. NWS HYDRO-17), Silver Spring, Maryland.

Baumgartner, A. 1981. 'Water Balance', Paper presented at the *World Climate Programme Study Conference on Land Surface Processes in Atmospheric General Circulation Models*. Also published in Eagleson, P. S. (ed.), 1982. *Land Surface Processes in Atmospheric General Circulation Models*, Cambridge University Press, New York.

Baumgartner, A. and Reichel, E. 1975. *The World Water Balance: Mean Annual Global, Continental and Maritime Precipitation, Evaporation and Runoff*, Elsevier, Amsterdam.

C. W. Thornthwaite Associates. 1954. 'Estimating soil tractionability from climatic data: final report', *Publications in Climatology*, **7**, 3.

Davies, J. A. and Allen, C. D. 1973. 'Equilibrium, potential and actual evaporation from cropped surfaces in southern Ontario', *Journal of Applied Meteorology*, **12**, 649.

de Jong, R. 1973. *Net Radiation Received by a Horizontal Surface on the Earth: A Literature Study Directed to Evapotranspiration Calculations*, Sijthoss and Noordhoff.

FitzGibbon, J. E. and Dunne, T. 1983. 'Influence of subarctic vegetation cover on snowmelt', *Physical Geography*, **4**, 61.

van Hylckama, T. E. A. 1956. 'The water balance of the Earth', *Publications in Climatology*, **9**, 59.

Jaeger, L. 1976. 'Monatskarten des Niederschlages für die ganze Erde', *Berichte Deutscher Wetterd*, NR. 139, Offenbach.

Jaeger, L. 1983. 'Monthly and areal patterns of mean global precipitation' in Street-Perrott, A. *et al.* (eds). *Variations in the Global Water Budget*, D. Reidel, Dordrecht, Holland

Jensen, M. E. (ed.) 1973. *Consumptive Use of Water and Irrigation Water Requirements*, American Society of Civil Engineers, New York.

Mather, J. R. 1962. 'Average climatic water balance data of the continents: part 1. Africa', *Publications in Climatology*, **15**, (2).

Mather, J. R. 1963a. 'Average climatic water balance data of the continents: part 2. Asia (excluding U.S.S.R.)', *Publications in Climatology*, **16**, (1).

Mather, J. R. 1963b. 'Average climatic water balance data of the continents: part 3. U.S.S.R.', *Publications in Climatology*, **16,** (2).
Mather, J. R. 1963c. 'Average climatic water balance data of the continents: part 4. Australia, New Zealand, and Oceania', *Publications in Climatology*, **16,** (3).
Mather, J. R. 1964a. 'Average climatic water balance data of the continents: part 5. Europe', *Publications in Climatology*, **17,** (1).
Mather, J. R. 1964b. 'Average climatic water balance data of the continents: part 6. North America (excluding United States)', *Publications in Climatology*, **17,** (2).
Mather, J. R. 1964c. 'Average climatic water balance data of the continents: part 7. United States', *Publications in Climatology*, **17,** (3).
Mather, J. R. 1965. 'Average climatic water balance data of the continents: part 8. South America', *Publications in Climatology*, **18,** (2).
McGuinness, J. L. and Bordne, E. F. 1971. *A Comparison of Lysimeter-Derived Potential Evapotranspiration with Computed Values*, USDA, Agricultural Research Service, Soil and Water Conservation Research Division, Corn Belt Branch, North Appalachian Experimental Watershed (ARS 41-), Coshocton, Ohio.
Mintz, Y. 1981. 'A brief review of the present status of global precipitation estimates' in Atlas, D. and Theile, O. W. (eds), *Report of the Workshop on Precipitation Measurements from Space*, NASA Goddard Space Flight Center, Greenbelt, Maryland, D. 1.
Mintz, Y. and Serafini, Y. 1984. 'Global fields of monthly normal soil moisture as derived from observed precipitation and an estimated evapotranspiration', *Final Scientific Report under NASA Grant No. NAS 5-26, Part V*, Department of Meteorology, University of Maryland, College Park, Maryland.
Möller, F. 1951. 'Vierteljahreskarten des Niederschlages', *Petermanns Geogr. Mitt.*, **95,** 1.
Mustonen, S. E. and McGuinness, J. L. 1968. *Estimating Evapotranspiration in a Humid Region*, USDA, Agricultural Research Service (Tech. Bulletin No. 1389), Washington, D.C.
Nappo, C. J. 1975. 'Parameterization of surface moisture and evaporation rate in a planetary boundary layer model', *Journal of Applied Meteorology*, **14,** 289.
Pelton, W. L., King, K. M. and Tanner, C. B. 1960. 'An evaluation of the Thornthwaite and mean temperature methods for determining potential evapotranspiration', *Agronomy Journal*, **52,** 387.
Priestley, C. H. B. and Taylor, R. J. 1972. 'On the assessment of surface heat flux and evaporation using large-scale parameters', *Mon. Wea. Rev.*, **100,** 81.
Pysklywec, D. W., Davar, K. S. and Bray, D. I. 1968. 'Snowmelt at an index plot', *Water Resources Research*, **4,** 937.
Spangler, W. M. L. and Jenne, R. L. 1984. *Reference Manual: World Monthly Surface Station Climatology*, National Center for Atmospheric Research, Boulder, Colorado.
Steinhauser, F. (Tech. Supervisor). 1979. *Climatic Atlas of North and Central America. I: Maps of Mean Temperature and Precipitation*, WMO (also UNESCO and Cartographia), Geneva.
Strahler, A. N. and Strahler, A. H. 1978. *Modern Physical Geography*, J. Wiley, New York.
Storr, D. 1978. *A Comparison of Daily Snowmelt Calculated by the U.S. Corps of Engineers Theoretical Model with Measured Amounts on a Snowpillow*, Storm Water Resources Consulting Service, Ganges, British Columbia.
Thornthwaite, C. W. 1948. 'An approach toward a rational classification of climate', *Geographical Review*, **38,** 55.
Thornthwaite, C. W. and Hare, F. K. 1965. 'The loss of water to the air', *Meteorological Monographs*, **28,** 163.
Thornthwaite, C. W. and Mather, J. R. 1955. 'The water balance', *Publications in Climatology*, **8,** (1).
Thornthwaite, C. W. and Mather, J. R. 1957. 'Instructions and tables for computing potential evapotranspiration and the water balance', *Publications in Climatology*, **10,** (3).
Thornthwaite, C. W., Mather, J. R. and Carter, D. B. 1958a. 'Three water balance maps of southwest Asia', *Publications in Climatology*, **11,** (1).
Thornthwaite, C. W., Mather, J. R. and Carter, D. B. 1958b. *Three water balance maps of Eastern North America*, Report prepared for Resources for the Future, Inc., Washington.
Wernstedt, F. L. 1972. *World Climatic Data*, Climatic Data Press, Lemont, Pennsylvania.
Willmott, C. J. 1977. 'WATBUG: A FORTRAN IV algorithm for calculating the climatic water budget', *Publications in Climatology*, **30,** (2).
Willmott, C. J. 1984. 'On the evaluation of model performance in physical geography' in Gaile, G. L. and Willmott, C. J. (eds). *Spatial Statistics and Models*, D. Reidel, Dordrecht, Holland.
Willmott, C. J., Mather, J. R. and Rowe, C. M. 1981. 'Average monthly and annual surface air temperature and precipitation data for the world. Part 1: the eastern hemisphere. Part 2: the western hemisphere', *Publications in Climatology*, **34,** (1) and (2).
Willmott, C. J., Rowe, C. M. and Philpot, W. D. 1985. 'Small-scale climate maps: a sensitivity analysis of some common assumptions associated with grid point interpolation and contouring', *The American Cartographer*, **12,** 5.
Wilm, H. G., Thornthwaite, C. W., Colman, E. A., Cummings, N. W., Croft, A. R., Gisborne, H. T., Harding, S. T., Hendrickson, A. H., Hoover, M. D., Houk, I. E., Kittredge, J., Lee, C. H., Rossby, C.-G., Saville, T., and Taylor, C. A. 1944. 'Report of the Committee on Transpiration and Evaporation, 1943--44', *Transactions, American Geophysical Union*, **25,** 683.